

# Finite volume treatment of $\pi\pi$ scattering and limits to phase shifts extraction from lattice QCD

M. Albaladejo<sup>1</sup>, J. A. Oller<sup>1</sup>, E. Oset<sup>2</sup>, G. Rios<sup>1</sup> and L. Roca<sup>1</sup>

<sup>1</sup>*Departamento de Física. Universidad de Murcia. E-30100 Murcia, Spain.*

<sup>2</sup>*Departamento de Física Teórica and IFIC, Centro Mixto Universidad de Valencia-CSIC, Institutos de Investigación de Paterna, Aptdo. 22085, 46071 Valencia, Spain.*

(Dated: January 22, 2018)

We study theoretically the effects of finite volume for  $\pi\pi$  scattering in order to extract physical observables for infinite volume from lattice QCD. We compare three different approaches for  $\pi\pi$  scattering (lowest order Bethe-Salpeter approach,  $N/D$  and inverse amplitude methods) with the aim to study the effects of the finite size of the box in the potential of the different theories, specially the left-hand cut contribution through loops in the crossed  $t, u$ -channels. We quantify the error made by neglecting these effects in usual extractions of physical observables from lattice QCD spectra. We conclude that for  $\pi\pi$  phase-shifts in the scalar-isoscalar channel up to 800 MeV this effect is negligible for box sizes bigger than  $2.5m_\pi^{-1}$  and of the order of 5% at around  $1.5 - 2m_\pi^{-1}$ . For isospin 2 the finite size effects can reach up to 10% for that energy. We also quantify the error made when using the standard Lüscher method to extract physical observables from lattice QCD, which is widely used in the literature but is an approximation of the one used in the present work.

## I. INTRODUCTION

One of the aims in present lattice QCD calculations is the determination of the hadron spectrum and many efforts are devoted to this task [1–19]. A recent review on the different methods used and results can be seen in [20]. Since one evaluates the spectrum for particles in a finite box, one must use a link from this spectrum to the physical one in infinite space. Sometimes, when it rarely happens, an energy of the box rather independent of the volume is taken as a proof that this is the energy of a state in the infinite volume space. In other works the “avoided level crossing”, with lines of spectra that get close to each other and then separate, is usually taken as a signal of a resonance, but this criteria has been shown insufficient for resonances with a large width [21–23]. A more accurate method consists on the use of Lüscher’s approach, but this works for resonances with only one decay channel. The method allows to reproduce the phase-shifts for the particles of this decay channel starting from the discrete energy levels in the box [24, 25]. This method has been recently simplified and improved in [23] by keeping the full relativistic two-body propagator (Lüscher’s approach keeps the imaginary part of this propagator exactly but makes approximations on the real part). The work of [23] also extends the method to two or more coupled channels. The extension to coupled channels has also been worked out in [26–28]. The work of [23] presents an independent method, which is rather practical, and has been tested and proved to work in realistic cases of likely lattice results. The method has been extended in [29] to obtain finite volume results from the Jülich model for the meson-baryon interaction and in [30] to study the interaction of the  $DK$  and  $\eta D_s$  system where the  $D_{s^*0}(2317)$  resonance is dynamically generated from the interaction of these particles. The case of the  $\kappa$  resonance in the  $K\pi$  channel is also addressed in [31] following the approach of Ref. [23]. It has also been

extended to the case of interaction of unstable particles in [32], to the study of the DN interaction [33], the  $\pi\pi$  interaction in the  $\rho$  channel [34] and to find strategies to determine the two  $\Lambda(1405)$  states from lattice results [35].

In Ref. [23] the problem of getting phase-shifts and resonances from lattice QCD results (“inverse problem”) using two coupled channels was addressed. Special attention was given to the evaluation of errors and the precision needed on the lattice QCD calculations to obtain phase-shifts and resonance properties with a desired accuracy. The derivation of the basic formula of [23] is done using the method of the chiral unitary approach [36] to obtain the scattering matrix from a potential. This method uses a dispersion relation for the inverse of the amplitude, taking the imaginary part of  $T^{-1}$  in the physical region and using unitarity in coupled channels [37, 38]. The method does not integrate explicitly over the left-hand cut singularity. Nevertheless, the latter might lead to interesting problems in finite volume calculations because in field theory, loops in the  $t$ - or  $u$ -channel that contribute to crossed cuts, are volume dependent. There is no problem to incorporate these extra terms into the chiral unitary approach by putting them properly in the interaction kernel of the Bethe Salpeter equation or  $N/D$  method [37, 39], or using the inverse amplitude method (IAM) [40, 41]. However, the method of [23] to analyze lattice spectra and obtain phase-shifts explicitly relies upon having a kernel in the Bethe Salpeter equation which is volume independent. The same handicap occurs in the use of the standard Lüscher approach, where contributions from possible volume dependence in the potential are shown to be “exponentially suppressed” in the box volume. Yet, there is no way, unless one knows precisely the source of the volume dependent terms, to estimate these effects and determine for which volumes the “exponentially suppressed” corrections have become smaller than a desired quantity. This is however an im-

portant information in realistic calculations. The purpose of the present paper is to address this problem in a practical case, the scattering of pions in  $s$ -wave. For that we determine the strength of these volume dependent terms as a function of the size of the box and the impact of these effects in the determination of the phase-shifts in the infinite volume case.

The contents of the paper are as follows. After this introduction, we summarize in Sec. II the three models used to evaluate  $\pi\pi$  scattering in the infinite and finite volume case. We then follow by studying the dependence on the lattice size of the box  $L$  of the resulting phase shifts in Sec. III. Conclusions are collected in Sec. IV.

## II. THE $\pi\pi$ SCATTERING IN THE FINITE BOX

In this section we explain the three models that we are going to consider in the present work to evaluate the  $\pi\pi$  scattering within the chiral unitary approach: lowest order Bethe-Salpeter (BS), N/D and Inverse amplitude method (IAM). The latter two provide contributions to the left-hand cut of the scattering amplitude while the BS does not. After summarizing the models for the infinite volume, we explain for each of them how to evaluate the scattering in a box of finite size  $L$ . We study the scalar channel up to total energies of about 800 MeV for both isospin ( $I$ ) 0 and 2. The isoscalar case is relevant for the lattice QCD studies of  $\sigma$  (or  $f_0(600)$  [42]) meson resonance, while for the isotensor case the left-hand cut is more relevant (see below). Up to those energies the  $K\bar{K}$  and  $\eta\eta$  channels in the  $I = 0$  case are negligible, hence, we deal here only with the  $\pi\pi$  channel.

### A. Lowest order Bethe-Salpeter approach

In the chiral unitary approach the scattering matrix can be given by the Bethe-Salpeter equation in its factorized form [43]

$$T = [1 - VG]^{-1}V = [V^{-1} - G]^{-1}, \quad (1)$$

where  $V$  is the  $\pi\pi$  potential,  $V = -\frac{1}{f_\pi^2}(s - \frac{m^2}{2})$  for  $I = 0$  and  $V = \frac{1}{2f_\pi^2}(s - 2m^2)$  for  $I = 2$ , which are obtained from the lowest order chiral Lagrangians [44], with  $m$  the pion mass and  $f_\pi = 92.4$  MeV. In Eq. (1)  $G$  is the loop function of two meson propagators, which is defined as

$$G = i \int \frac{d^4p}{(2\pi)^4} \frac{1}{(P-p)^2 - m^2 + i\epsilon} \frac{1}{p^2 - m^2 + i\epsilon}, \quad (2)$$

with  $P$  the four-momentum of the global meson-meson system. Note that Eq. (1) only has right-hand cut, unlike the other two approaches discussed in the next subsections.

The loop function in Eq. (2) can be regularized either with dimensional regularization or with a three-momentum cutoff. The connection between both methods was shown in Refs. [38, 41]. In dimensional regularization<sup>1</sup> the integral of Eq. (2),  $G^D$ , is evaluated and gives for the  $\pi\pi$  system [38, 45]

$$G^D(E) = \frac{1}{(4\pi)^2} \left\{ a(\mu) + \log \frac{m^2}{\mu^2} + \sigma \log \frac{\sigma + 1}{\sigma - 1} \right\}, \quad (3)$$

where  $\sigma = \sqrt{1 - \frac{4m^2}{s}}$ ,  $s = E^2$ , with  $E$  the energy of the system in the center of mass frame,  $\mu$  is a renormalization scale and  $a(\mu)$  is a subtraction constant (note that only the combination  $a(\mu) - \log \mu^2$  is the relevant degree of freedom, that is, there is only one independent parameter).

The loop function  $G$  can also be regularized with a three momentum cutoff  $p_{\max}$  and, after the  $p^0$  integration is performed [43], it results

$$G(s) = \int_{|\vec{p}| < p_{\max}} \frac{d^3\vec{p}}{(2\pi)^3} \frac{1}{\omega(\vec{p})} \frac{1}{s - 4\omega(\vec{p})^2 + i\epsilon},$$

$$\omega(\vec{p}) = \sqrt{m^2 + \vec{p}^2}. \quad (4)$$

Let us now address the modifications in order to evaluate the  $\pi\pi$  scattering in a finite box following the procedure explained in Ref. [23]. The main difference with respect to the infinite volume case is that instead of integrating over the energy states of the continuum with  $\vec{p}$  being a continuous variable as in Eq. (4), one must sum over the discrete momenta allowed in a finite box of side  $L$  with periodic boundary conditions. We then have to replace  $G$  by  $\tilde{G}$ , where

$$\tilde{G} = \frac{1}{L^3} \sum_{\vec{p}}^{|\vec{p}| < p_{\max}} \frac{1}{\omega(\vec{p})} \frac{1}{s - 4\omega(\vec{p})^2},$$

$$\vec{p} = \frac{2\pi}{L} \vec{n}, \quad \vec{n} \in \mathbb{Z}^3 \quad (5)$$

For the sake of comparison with the other models considered in the present work, where dimensional regularization is always done, we use the procedure of [30] in order to write the finite volume loop function  $\tilde{G}$  in terms

---

<sup>1</sup> In our context we refer to the  $G$  function given in Eq. (3) as calculated in “dimensional regularization”. Of course, with the latter procedure the results is infinite. The infinite is removed by the subtraction constant  $a(\mu)$ . A more accurate formulation can be given in terms of dispersion relations, the interested reader on this point can consult Refs. [37, 38], though the final result is the same.

of the infinite volume one  $G^D$  evaluated in dimensional regularization:

$$\tilde{G} = G^D + \lim_{p_{\max} \rightarrow \infty} \left[ \frac{1}{L^3} \sum_{p_i}^{p_{\max}} I(p_i, s) - \int_{p < p_{\max}} \frac{d^3 p}{(2\pi)^3} I(p, s) \right], \quad (6)$$

where  $I(p, s)$  is the integrand of Eq. (4)

$$I(p, s) = \frac{1}{\omega(\vec{p})} \frac{1}{s - 4\omega(\vec{p})^2}. \quad (7)$$

Note that  $\tilde{G}$  of Eq. (6) depends on the subtraction constant  $a$  instead of the three-momentum cutoff  $p_{\max}$ .

In the box the scattering matrix reads

$$\tilde{T} = \frac{1}{V^{-1} - \tilde{G}}. \quad (8)$$

The eigenenergies of the box correspond to energies that produce poles in the  $\tilde{T}$  matrix, which corresponds to the condition  $\tilde{G}(E) = V^{-1}(E)$ . Therefore for those values of the energies, the  $T$  matrix for infinite volume can be obtained by

$$T(E) = (V^{-1}(E) - G(E))^{-1} = (\tilde{G}(E) - G(E))^{-1}. \quad (9)$$

The amplitude is related to the phase-shifts by

$$T(E) = -\frac{8\pi E}{p} \frac{1}{\cot \delta - i}, \quad (10)$$

where  $p = \frac{E}{2} \sqrt{1 - \frac{4m^2}{s}}$  is the CM momentum.

Eq. (9) is nothing but Lüscher formula [24, 25] except that, as shown in Ref. [23], Eq. (9) keeps all the terms of the relativistic two-body propagator, while Lüscher's approach neglects terms in  $\text{Re } I(p)$  which are exponentially suppressed in the physical region, but can become sizable below threshold, or in other cases when small volumes are used or large energies are involved.

## B. The IAM approach

The next approach considered is the elastic Inverse Amplitude Method (IAM) [40], which we briefly review in this section and describe how to extend it to consider scattering in a finite box.

The elastic IAM makes use of elastic unitarity and Chiral Perturbation Theory (ChPT) [44] to evaluate a dispersion relation for the inverse of the  $\pi\pi$  scattering partial wave of definite isospin  $I$  and angular momentum  $J$ ,  $T^{IJ}$  (in the following we drop the superscript  $IJ$  to simplify notation). The advantage of using the inverse

of a partial wave stems from the fact that its imaginary part is fixed by unitarity,

$$\text{Im } T = -\frac{\sigma}{16\pi} |T|^2 \Rightarrow \text{Im } T^{-1} = \frac{\sigma}{16\pi}. \quad (11)$$

Thus, the right-hand cut integral can be evaluated exactly in the elastic regime and the obtained partial wave satisfies unitarity exactly. The partial wave amplitudes calculated in ChPT cannot satisfy unitarity exactly since they are obtained in a perturbative expansion  $T = T_2 + T_4 + \mathcal{O}(p^6)$ , where  $T_2 = \mathcal{O}(p^2)$  and  $T_4 = \mathcal{O}(p^4)$  are the Leading Order and Next-to-Leading Order contributions in the chiral expansion of  $T$ , respectively. However, unitarity is satisfied in a perturbative way,

$$\text{Im } T_2 = 0, \quad \text{Im } T_4 = -\frac{\sigma}{16\pi} T_2^2, \quad \dots \quad (12)$$

These equations allow us to evaluate the dispersion relation and obtain a compact form for the partial wave as we show below.

We write then a dispersion relation for an auxiliary function  $F \equiv T_2^2/T$ , whose analytic structure consists on a right-hand cut ( $RC$ ) from  $4m_\pi^2$  to  $\infty$ , a left-hand cut ( $LC$ ) from  $-\infty$  to 0, and possible poles coming from zeros of  $T$ ,

$$F(s) = F(0) + F'(0)s + \frac{1}{2}F''(0)s^2 + \frac{s^3}{\pi} \int_{RC} ds' \frac{\text{Im } F(s')}{s'^3(s' - s)} + LC(F) + PC, \quad (13)$$

where we have performed three subtractions to ensure convergence. In the above equation  $LC(F)$  stands for the integral over the left-hand cut, and  $PC$  stands for possible poles contributions, which are present in the scalar waves due to the Adler zeros. Using Eqs. (11) and (12) we can evaluate *exactly* in the  $RC$  integral  $\text{Im } F = -\text{Im } T_4$ , and obtain for the right-hand cut  $RC(F) = -RC(T_4)$ . The subtraction constants can be evaluated with ChPT since they only involve amplitudes or their derivatives evaluated at  $s = 0$ ,  $F(0) \simeq T_2(0) - T_4(0)$ ,  $F'(0) \simeq T_2'(0) - T_4'(0)$ ,  $F''(0) \simeq -T_4''(0)$ . The left-hand cut can be considered to be dominated by its low energy part, since we have three subtractions, and it is also damped by an extra  $1/(s' - s)$  when considering physical values of  $s$ . Then, we evaluate it using ChPT to obtain  $LC(F) \simeq -LC(T_4)$ . The pole contribution is formally  $\mathcal{O}(p^6)$  and we neglect it (this causes some technical problems in the subthreshold region around the Adler zeros which can be easily solved, but they do not affect the description of scattering or resonances, for details see [46]). Taking into account all the above considerations we arrive at

$$\begin{aligned} \frac{T_2^2(s)}{T(s)} &\simeq T_2(0) + T_2'(0)s - T_4(0) - T_4'(0)s - \frac{1}{2}T_4''(0)s^2 \\ &\quad - RC(T_4) - LC(T_4) = T_2(s) - T_4(s), \end{aligned} \quad (14)$$

where in the last step we have taken into account that  $T_2(s)$  is just a first order polynomial in  $s$  so that  $T_2(s) = T_2(0) + T_2'(0)s$ , and that the remaining piece in the middle member of Eq. (14) is a dispersion relation for  $-T_4(s)$ . Then one obtains the simple IAM formula,

$$T^{IAM} = \frac{T_2^2}{T_2 - T_4}. \quad (15)$$

This formula can be systematically extended to higher orders by evaluating the subtraction constants and the left-hand cut in the dispersion relation to higher orders. Note that the full one-loop ChPT calculation is used, so the IAM partial waves depend on the chiral Low Energy Constants (LECs), that absorb the loop divergences through their renormalization and depend on a renormalization scale  $\mu$ . Of course, this  $\mu$  dependence is canceled out in physical observables. In the case of  $\pi\pi$  scattering there appear four LECs, denoted  $l_i^r(\mu)$ ,  $i = 1 \dots 4$ . These LECs are not fixed from symmetry considerations and their value has to be determined from experiment. For the IAM calculations here we take the values used in [47]:  $10^3 l_1^r = -3.7 \pm 0.2$ ,  $10^3 l_2^r = 5.0 \pm 0.4$ ,  $10^3 l_3^r = 0.8 \pm 3.8$ ,  $10^3 l_4^r = 6.2 \pm 5.7$ , at  $\mu = 770$  MeV, which give a good description of phase-shift data. Note that in the present work we are not interested in a detailed description of scattering data, but on the effects of ignoring the exponentially suppressed dependence on the box size when using Lüscher's or the chiral unitary approach to obtain the scattering phase-shifts from the energy levels in finite volume.

To evaluate the IAM partial waves in a finite box of size  $L$  we proceed in a similar way as in subsection II A. The only piece we need to change is  $T_4$ , that receives contributions from loop diagrams, whose momentum integrals should be replaced by discrete sums over the allowed momenta in the finite box.

Let us first note that the  $\mathcal{O}(p^4)$  contribution to the  $\pi\pi$  scattering amplitude  $A_4(s, t, u)$ , where the partial wave amplitude at the same order ( $T_4^{JJ}(s)$ ) is obtained by projecting  $A_4(s, t, u)$  on isospin  $I$  and angular momentum  $J$ , has the form [44]

$$A_4(s, t, u) = B(s, t, u) + C(s, t, u), \quad (16)$$

where  $C(s, t, u)$  is a second order polynomial in  $s$ ,  $t$ , and  $u$  which contains the LECs. On the other hand,  $B(s, t, u)$  contains the non-analyticities coming from the one-loop diagrams with vertices from the  $\mathcal{O}(p^2)$  Lagrangian,

$$\begin{aligned} B(s, t, u) = & \frac{1}{6f_\pi^4} \left[ 3(s^2 - m_\pi^4) \bar{G}(s) \right. \\ & + \{t(t-u) - 2m_\pi^2 t + 4m_\pi^2 u - 2m_\pi^4\} \bar{G}(t) \\ & \left. + \{u(u-t) - 2m_\pi^2 u + 4m_\pi^2 t - 2m_\pi^4\} \bar{G}(u) \right], \end{aligned} \quad (17)$$

with

$$\bar{G}(s) = \frac{1}{16\pi^2} \left( \sigma(s) \log \frac{\sigma(s) + 1}{\sigma(s) - 1} - 2 \right), \quad (18)$$

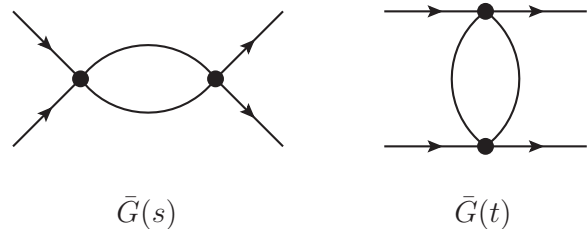


FIG. 1. Pion loops in the  $s$  (left) and  $t$  (right) channels contributing to the  $\mathcal{O}(p^4)$  chiral  $\pi\pi$  scattering amplitude  $A_4(s, t, u)$ . The  $s$ -channel loop gives rise to the right unitarity cut, whereas the  $t$ -channel (as well as  $u$ -channel) loop contributes to the left-hand cut in the partial wave.

where we have defined  $\bar{G}(s) \equiv G(s) - G(0)$ .<sup>2</sup>  $G(s)$  is the loop function of two pions, Eq. (2) with  $s = P^2$ . There are three loop function contributions, proportional to  $\bar{G}(s)$ ,  $\bar{G}(t)$  and  $\bar{G}(u)$ , each one coming from a pion loop in the  $s$ ,  $t$  and  $u$ -channels respectively, as schematically shown in Fig. 1. The  $s$ -channel loops are responsible for the right unitarity cut, and contain the most important  $L$  dependence of the amplitude. This  $L$  dependence coming from the unitarity cut is the one used by the Lüscher/chiral unitary approach method to obtain the phase-shift from the energy levels in a finite volume. However, the  $t$  and  $u$ -channel loops, which give rise to the left-hand cut when projecting into partial waves, give an extra dependence on  $L$  (polarization corrections in the terminology of Ref. [25]) that is neglected in the Lüscher/chiral unitary approach method since it is exponentially suppressed.

Then, to obtain the IAM amplitudes in finite volume we have to replace  $T_4(s)$  in Eq. (15) with  $\tilde{T}_4(s)$ , which is obtained projecting into the corresponding partial wave the  $\pi\pi$  scattering amplitude in finite volume  $\tilde{A}_4(s, t, u)$ , obtained from Eq. (16) but replacing the loop functions in Eq. (17) with their finite volume counterparts,  $\bar{G}_{FV}$ . Following again the procedure in [30], the finite volume loop functions are obtained from the infinite volume ones by

$$\begin{aligned} \bar{G}_{FV}(z) = & \bar{G}(z) + \lim_{p_{\max} \rightarrow \infty} \left[ \frac{1}{L^3} \sum_{p_i}^{p_{\max}} I(p_i, z) \right. \\ & \left. - \int_{p < p_{\max}} \frac{d^3 p}{(2\pi)^3} I(p, z) \right], \end{aligned} \quad (19)$$

with  $z = s, t$  or  $u$ . Now, the energy levels in the box are obtained from the poles in the scattering partial wave (15), or equivalently, the zeros of  $T_2(s) - \tilde{T}_4(s)$ .

<sup>2</sup> This  $\bar{G}$  relates to the  $\bar{J}$  used in [44] as  $\bar{J} = -\bar{G}$ , in accordance with our normalization, where the amplitudes have opposite sign to those in [44].

From these energy levels at several values of  $L$  one can re-obtain the phase-shifts for the infinite volume with the Lüscher/chiral unitary approach method, and compare them with the exact infinite volume result to quantify the effect of neglecting the  $L$  dependence coming from the left-hand cut.

### C. The N/D method

The case presented in subsection IIA, can be put in the more general framework of the N/D method [37, 38, 48, 49]. The amplitude was denoted by  $T(s)$  in Eq. (1). This master formula is obtained by solving algebraically the N/D method [37, 38, 48, 50], with the crossed cuts treated perturbatively, while the right-hand cut is resummed exactly. The different chiral orders of  $V(s) = V_2(s) + V_4(s) + \dots$  are calculated by matching  $T(s)$  with the perturbative amplitudes  $T_n(s)$ . In this way, up to  $\mathcal{O}(p^4)$ ,

$$\begin{aligned} T(s) &= \frac{V(s)}{1 - V(s)G(s)} \\ &= T_2(s) + T_4(s) + \dots \\ &= V_2(s) + V_4(s) + V_2(s)^2 G(s) + \dots, \end{aligned} \quad (20)$$

where the ellipsis indicates  $\mathcal{O}(p^6)$  and higher orders in the expansion. It results then:

$$\begin{aligned} V_2(s) &= T_2(s), \\ V_4(s) &= T_4(s) - T_2(s)^2 G(s). \end{aligned} \quad (21)$$

The finite piece of the unitarity term in the  $\pi\pi$  chiral amplitude is given by:

$$T_4^U(s) = T_2(s)^2 \bar{G}(s), \quad (22)$$

with  $\bar{G}(s)$  given in Eq. (18). In this way, the kernel  $V(s) = V_2(s) + V_4(s)$  has no unitarity cut because:

$$T_4^U(s) - T_2(s)^2 G(s) = T_2(s)^2 (\bar{G}(s) - G(s)), \quad (23)$$

and the cut is cancelled in the r.h.s. of the previous equation. The full right-hand cut stems then from the denominator  $1 - V(s)G(s)$  in Eq. (1).

In the infinite volume case, the LECs are fixed to the experiment, as well as the subtraction constant  $a$ . We use here the central values of the fit given in [51], for which the values of the finite and scale independent LECs  $\bar{l}_i$  are  $\bar{l}_1 = 0.8 \pm 0.9$ ,  $\bar{l}_2 = 4.6 \pm 0.4$ ,  $\bar{l}_3 = 2 \pm 4$ ,  $\bar{l}_4 = 3.9 \pm 0.5$ . In terms of the latter, the so-called renormalized LECs, which depend on the renormalization scale, are  $10^3 l_1^r = -2.8 \pm 0.9$ ,  $10^3 l_2^r = 2.5 \pm 0.8$ ,  $10^3 l_3^r = 2 \pm 6$ ,  $10^3 l_4^r = 3 \pm 3$ , where the renormalization scale is chosen as  $\mu = 770$  MeV. The subtraction constant  $a$  takes the value  $a = -1.2 \pm 0.4$ . We additionally note here that the same subtraction constant is used for both channels, as required by isospin symmetry [52].

In order to study the finite volume scattering, the same replacements as in the IAM and BS methods must be done. In particular, in the kernel  $V(s) \rightarrow \tilde{V}(s)$  no change is needed in  $V_2(s)$ , whereas  $V_4(s)$  is changed to  $\tilde{V}_4(s)$ ,

$$\tilde{V}_4(s) = \tilde{T}_4(s) - T_2(s)^2 \tilde{G}(s). \quad (24)$$

Notice that, in view of Eq. (23), there is no effect in the  $s$ -channel contributions to the kernel  $\tilde{V}(s)$ . The volume dependence enters then in the kernel through the  $t$ - and  $u$ -channel loop functions, where the replacement  $\bar{G}(z) \rightarrow \bar{G}_{FV}(z)$  in Eq. (19) for  $z = t, u$  must be done. The  $s$ -channel volume-dependence enters then at the denominator of the amplitude  $\tilde{T}(s) = \tilde{V}(s)/(1 - \tilde{V}(s)\tilde{G}(s))$  through the function  $\tilde{G}(s)$ , Eq. (6), which gives the most important contribution to the aforementioned dependence, as in the case of the IAM method.

## III. RESULTS

As already explained, the main aim of the present work is to quantify the effect of the dependence of the different potentials considered on the size of the box,  $L$ . Hence, we are going to compare the  $L$  dependence of the N/D and the IAM method with that of the BS, which kernel does not depend on  $L$ .

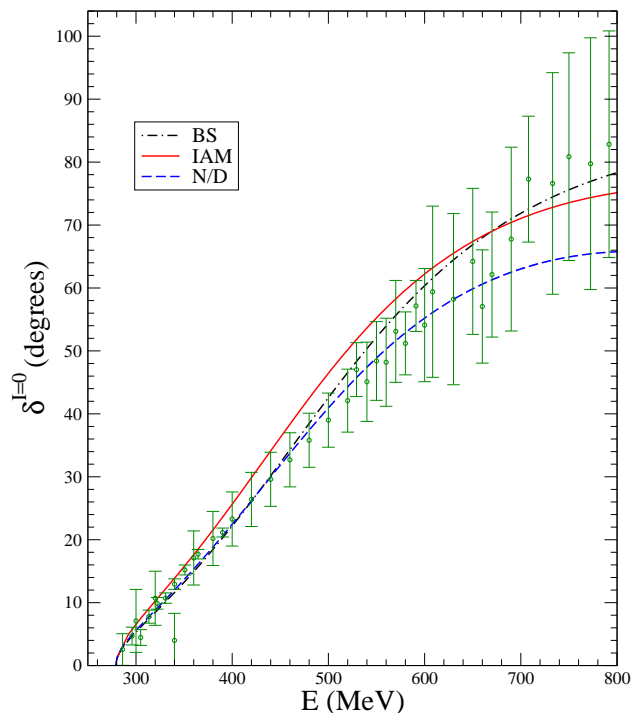


FIG. 2. Isospin  $I=0$ ,  $s$ -wave,  $\pi\pi \rightarrow \pi\pi$  phase-shifts for the three different models considered: solid, dashed and dot-dashed lines correspond to IAM, N/D and BS, respectively. The experimental data are from Refs. [53–57].

First we show in Fig. 2 the results for the  $\pi\pi$  phase-shifts in s-wave and  $I = 0$  for the three different models in infinite volume. The IAM and N/D results (solid and dashed lines, respectively) are the fits explained in the previous section and the BS (dot-dashed line) is fitted in this work to the experimental data [53–57] shown in the figure up to 800 MeV. The IAM and N/D approaches are essentially equivalent at low energies but differ slightly as the energy increases. Thus the difference between the IAM and N/D phase shifts is mainly due to the different set of data used in the fit and it also gives an idea of the theoretical uncertainty. The BS approach produces a curve in between the other two, closer to the N/D at low energies and to the IAM at higher energies. In any case, the different models are compatible within the experimental uncertainties. Let us note that what matters for the discussions in the present work is not the actual values of the phase-shifts at infinite volume but the relative change when going to the finite box.

In Fig. 3 we show the energy levels for different values of the cubic box size,  $L$ , for the different models which have been obtained from the zeroes of the scattering amplitudes in the finite box as explained in the previous section. The dotted lines represent the free  $\pi\pi$  energies in the box, while the others lines correspond to IAM, N/D and BS as in Fig. 2.

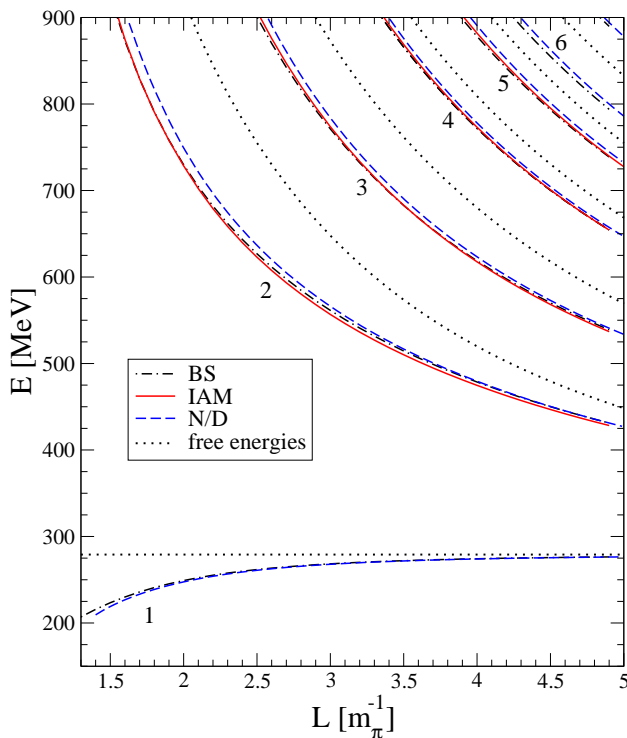


FIG. 3. The first energy levels as a function of the cubic box size  $L$  for the three different models considered for  $I = 0$ . The dotted lines indicate the free  $\pi\pi$  energies in the box. The rest of the lines correspond to IAM, N/D and BS as in Fig. 2.

The differences are very small for the largest values of

$L$  shown in the plot but are more important for smaller values of  $L$ , specially between the N/D and IAM methods. The BS approach produces a curve in between the other two, closer to the N/D. The IAM and BS are more similar for larger values of energies as can also be seen in the phase shifts, Fig. 2. As an example of small  $L$ , we note that for  $L = 1.7m_\pi^{-1}$  the difference between N/D and IAM is about 30 MeV.

An actual lattice calculation would provide some points over analogous trajectories in the  $E$  vs.  $L$  plots. The “inverse problem” is the problem of getting the actual scattering amplitudes (and hence by-product magnitudes like phase-shifts) in the infinite space from data produced by lattice QCD consisting of points in plots of  $E$  vs.  $L$  over the energy levels in the box. For points in these levels the amplitude in the infinite volume can be extracted from the generalization of the Lüscher formula, as explained in the previous sections,

$$T(E) = \frac{1}{\tilde{G}(E) - G(E)}. \quad (25)$$

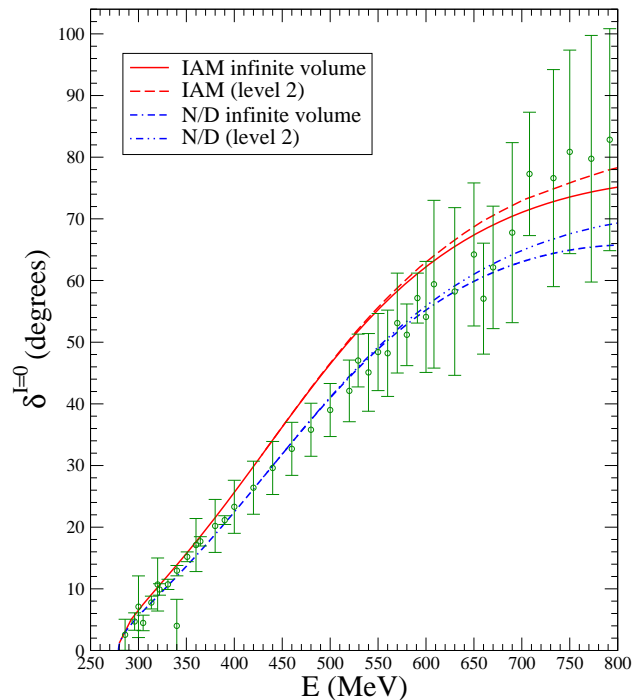


FIG. 4. Solution of the inverse problem for  $I = 0$  for the IAM and N/D methods. The BS result is the same as in the infinite volume case and thus we do not show it in the figure. We show the results obtained only from level 2 of Fig. 3 since the results with levels  $> 2$  almost overlap with the infinite volume line. For the meaning of each line consult the inset in the figure.

In Fig. 4 we show the phase-shifts obtained for the different methods implementing the “inverse problem” analysis (or “reconstructed” results) with Eq. (25) and from the  $E$  vs.  $L$  plot. For the *BS* model the results are

independent of the level used for a given  $E$ , since the potential does not depend on  $L$ , and they are equal to the infinite volume result. Therefore we do not show the BS result since it is the same as in Fig. 2. For the IAM and N/D methods the results depend on the level chosen for a given  $E$  since the potentials depend on  $L$  as explained in the previous sections. Actually, for levels  $> 2$  of Fig. 3 the results are almost equal to the infinite volume results and hence we do not show them in the figure since they would almost overlap with the infinite volume line. This is because, as seen in Fig. 3, for the higher energies these levels imply large values of  $L$ . Indeed, for energies below 800 MeV this implies values of  $L$  higher than about  $3m_\pi^{-1}$ . For the results obtained with level 2, the phase-shifts differ in about 5% of the result in the infinite volume at the higher energies considered. For  $E \sim 800$  MeV this implies  $L$  values slightly smaller than  $2m_\pi^{-1}$ , as can be seen in Fig. 3. It is worth noting that the effect of the dependence on  $L$  of the models with left-hand cut go in the same direction and are of similar size in spite of the different models used. This gives us confidence that the actual  $L$  dependence of the left-hand cut is properly considered and the real effect of any realistic model would be of the order obtained in the present work. An analysis with Eq. (25) applied to actual lattice results of  $E$  versus  $L$  levels would neglect the possible  $L$  dependence of the potential and hence the errors from the  $L$  dependence of the left-hand cut would be of the order of the differences shown in the figure. Note also that the  $L$  dependence of the results are smaller than the initial difference between the N/D and IAM themselves and also lower than the experimental uncertainties. Therefore, an actual lattice calculation should care about this  $L$  dependence only if it aims at getting errors smaller than the effect obtained in the present work.

In Figs. 5, 6 and 7 we show for the  $I = 2$  case the same results as in Figs. 2 to 4 for  $I = 0$ . In Fig. 5 we see that the IAM and N/D methods provide very similar results and compatible with the experimental data while the BS approach gets worse phase-shifts. This is because in the IAM and N/D the left-hand cut is included perturbatively order by order, unlike the BS model, and in this channel the left-hand cut is more relevant. In Fig. 6 we show the energy levels in the box for this channel.

Now both IAM and N/D provide similar results. In Fig. 7 we show the solution of the inverse problem for the phase-shifts. We see that the N/D method provides a higher  $L$  dependence for large values of the energies, unlike IAM. At 800 MeV the difference is about 10% for the N/D and 2% for the IAM. The difference in the phase-shifts between the two approaches is large in spite of the energy levels being very similar. This is because the energy levels are very close to the free case, unlike the  $I = 0$  case, and then the  $\tilde{G}$  function is very steep. This makes that small variations in  $E$  provide large variations in  $\tilde{G}$ .

In usual inverse problem analysis from actual lattice results, it is common to use the Lüscher formula [24, 25] which, as explained in section II A, is an approximation

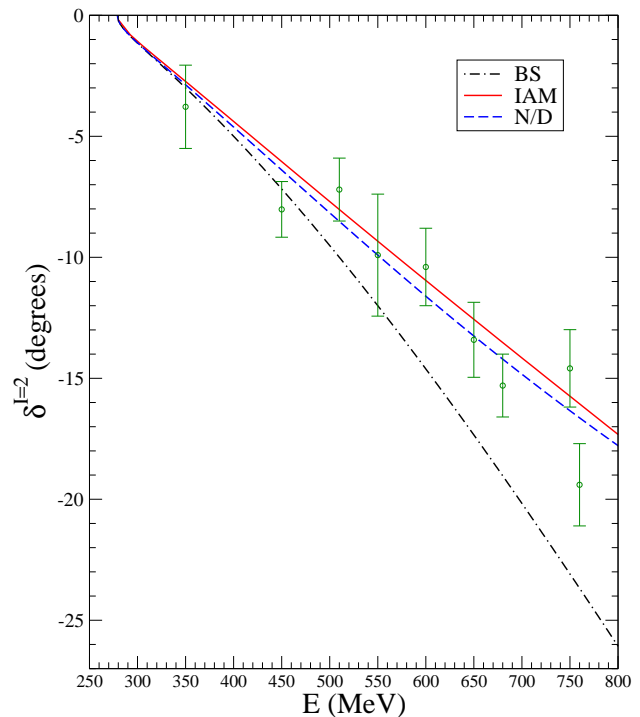


FIG. 5. Isospin  $I=2$ , s-wave,  $\pi\pi \rightarrow \pi\pi$  phase-shifts for the three different models considered. The experimental data are from Refs. [58, 59]. See the inset in the figure for the correspondence between the different lines and the approach used.

to that used in the present work, Eq. (9). Therefore it is worth studying what is the error made in the reconstructed phase-shifts if one uses the Lüscher equation instead of the exact one. In Ref. [23] it was shown that the Lüscher method can be reproduced if in Eq. (7) one substitutes

$$I(p, s) = \frac{1}{\omega(\vec{p})} \frac{1}{s - 4\omega(\vec{p})^2}. \quad (26)$$

by

$$I(p, s) = \frac{1}{2\sqrt{s}} \frac{1}{p_{\text{ON}}^2 - \vec{p}^2}. \quad (27)$$

where  $p_{\text{ON}} = \frac{E}{2} \sqrt{1 - \frac{4m^2}{s}}$ .

In Fig. 8 we show the effect in the isospin 0 phase-shifts of using the pure Lüscher method, Eq. (27), instead of the exact one, Eq. (26). (For the isospin 2 case the effect is small and thus we do not show any plot.) The difference is significant only for phase-shifts extracted from level 2 of Fig. 3 since the difference is only relevant for small values of  $L$ . Therefore we only plot results extracted from level 2. The difference between the exact method and the Lüscher one is similar for all the three different models for the potential. The size of the difference is similar to the one from the  $L$  dependence of the potential discussed above but goes in the opposite direction. Therefore they tend to compensate each other by chance.

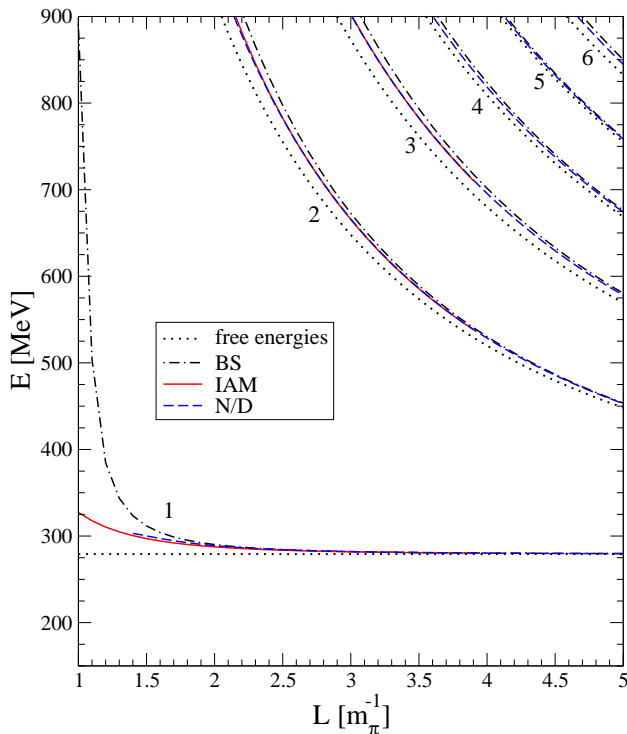


FIG. 6. The first energy levels as a function of the cubic box size  $L$  for the three different models considered for  $I = 2$ . The meaning of the different lines is as in Fig. 3.

#### IV. SUMMARY

In this paper we have faced for the first time in the literature the problem of the presence of the left-hand cut of the  $\pi\pi$  amplitude for the evaluation of phase-shifts from lattice QCD results using Lüscher's approach. The  $t$ - and  $u$ -channel terms can be taken into account in a field theoretical approach by means of the IAM, or N/D NLO methods, leading to good reproductions of the scattering data. Results from lattice QCD should contain all the dynamics and, as a consequence, should account for these effects too. However, the method to go from the discrete energy level in a box from lattice simulations to the phase shifts for scattering in the infinite volume case requires the use of Lüscher's approach, or its improved version of [23], both of which rely upon the existence of a volume independent potential. Yet, the terms contributing to the left-hand cut, containing loops in the  $t$ - and  $u$ -channels, are explicitly volume dependent. In this work we have investigated the errors induced by making use of [24] or [23] in the reproduction of phase-shifts from the energy spectra of lattice calculations in the finite box. We have found that in the case of  $\pi\pi$  scattering in  $s$ -wave, both for  $I = 0$  and  $I = 2$ , the effect of the  $L$  dependence in the potential is smaller than the typical errors from the experimental phase-shifts or the differences between the three models that we have used, the IAM, N/D NLO and

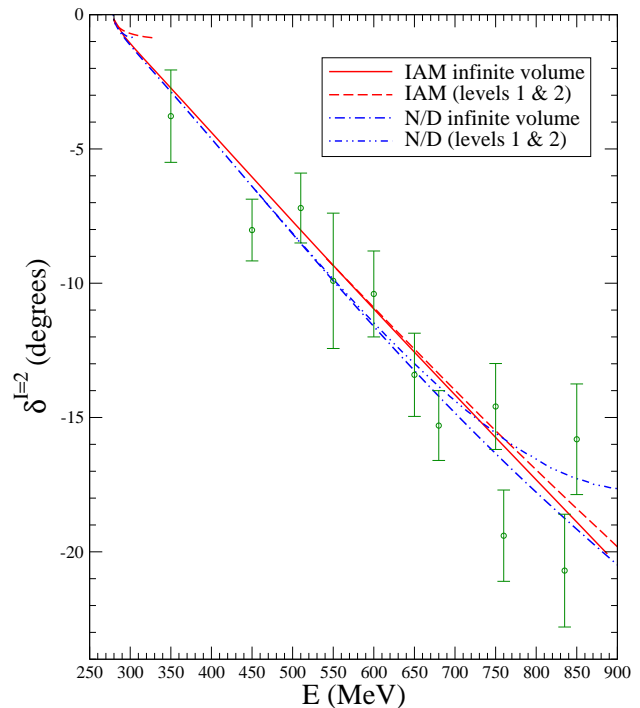


FIG. 7. Solution of the inverse scattering problem with  $I = 2$  for the IAM and N/D methods. The BS result is the same as in the infinite volume case and thus we do not show it in the figure. We show the results obtained only from level 1 and 2 of Fig. 6 since the results with levels  $> 2$  almost overlap with the infinite volume line. For the meaning of the lines consult the inset in the figure.

BS LO. This is good news for lattice calculations since one of the warnings not to go to small values of  $L$  was the possible  $L$  dependence of the potential which in some cases, like in the present one, we know that exists. We found that it is quite safe to ignore this dependence for  $L > 2.5m_\pi^{-1}$ , and even with values of  $L$  around  $1.5-2m_\pi^{-1}$  the errors induced are of the order of 5%.

On the other hand we have quantified the error made by using the pure Lüscher formula instead of the exact one, Eq. (25). The effect in the phase-shifts of this approximation tends to compensate, by chance, the effect of neglecting the  $L$  dependence in the potential discussed so far.

All these findings, together with the use of the approach of [23] that also eliminates  $L$  depended terms (exponentially suppressed) from the Lüscher's approach, can encourage the performance of lattice calculations with smaller size boxes with the consequent economy in the computing time.

#### ACKNOWLEDGMENTS

This work is partly supported by DGICYT contracts FIS2006-03438, the Generalitat Valenciana in the pro-



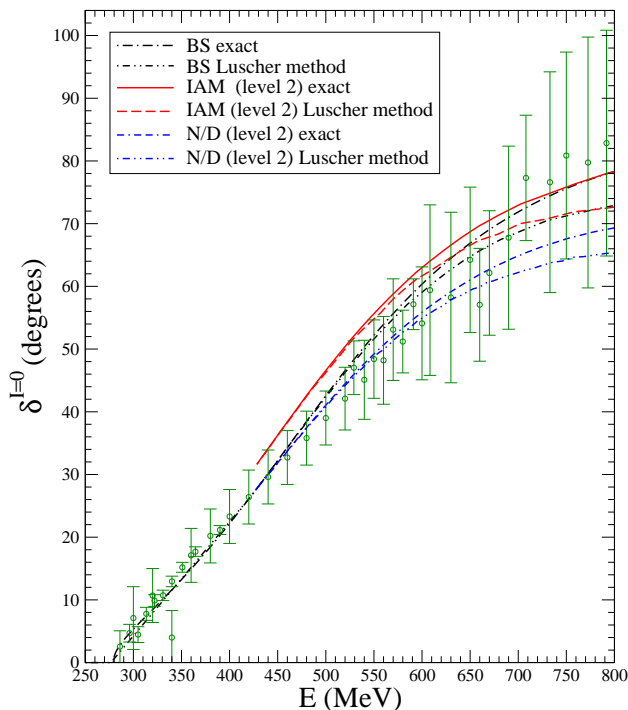


FIG. 8. Difference between the exact inverse method formula, Eq. (9), and the approximated Lüscher formula. The approach corresponding to each line is given in the inset in the figure.

- 
- [1] Y. Nakahara, M. Asakawa, T. Hatsuda, Phys. Rev. D **60** (1999) 091503.  
K. Sasaki, S. Sasaki and T. Hatsuda, Phys. Lett. B **623** (2005) 208.
- [2] N. Mathur, A. Alexandru, Y. Chen *et al.*, Phys. Rev. D **76** (2007) 114505.
- [3] S. Basak, R. G. Edwards, G. T. Fleming *et al.*, Phys. Rev. D **76** (2007) 074504.
- [4] J. Bulava, R. G. Edwards, E. Engelson *et al.*, Phys. Rev. D **82** (2010) 014507.
- [5] C. Morningstar, A. Bell, J. Bulava *et al.*, AIP Conf. Proc. **1257** (2010) 779.
- [6] J. Foley, J. Bulava, K. J. Juge *et al.*, AIP Conf. Proc. **1257** (2010) 789.
- [7] M. G. Alford and R. L. Jaffe, Nucl. Phys. B **578** (2000) 367.
- [8] T. Kunihiro, S. Muroya, A. Nakamura, C. Nonaka, M. Sekiguchi and H. Wada [SCALAR Collaboration], Phys. Rev. D **70** (2004) 034504.
- [9] F. Okiharu *et al.*, arXiv:hep-ph/0507187.  
H. Suganuma, K. Tsumura, N. Ishii and F. Okiharu, PoS **LAT2005** (2006) 070; Prog. Theor. Phys. Suppl. **168** (2007) 168.
- [10] C. McNeile and C. Michael [UKQCD Collaboration], Phys. Rev. D **74** (2006) 014508; A. Hart, C. McNeile, C. Michael and J. Pickavance [UKQCD Collaboration], Phys. Rev. D **74** (2006) 114504.
- [11] H. Wada, T. Kunihiro, S. Muroya, A. Nakamura, C. Nonaka and M. Sekiguchi, Phys. Lett. B **652** (2007) 250.
- [12] S. Prelovsek, C. Dawson, T. Izubuchi, K. Orginos and A. Soni, Phys. Rev. D **70** (2004) 094503; S. Prelovsek, T. Draper, C. B. Lang, M. Limmer, K. F. Liu, N. Mathur and D. Mohler, Conf. Proc. C **0908171** (2009) 508; Phys. Rev. D **82** (2010) 094507.
- [13] H.-W. Lin *et al.* [Hadron Spectrum Collaboration], Phys. Rev. D **79** (2009) 034502.
- [14] C. Gattlinger, C. Hagen, C. B. Lang, M. Limmer, D. Mohler and A. Schafer, Phys. Rev. D **79** (2009) 054501.
- [15] G. P. Engel *et al.* [BGR (Bern-Graz-Regensburg) Collaboration], Phys. Rev. D **82** (2010) 034505.
- [16] M. S. Mahbub, W. Kamleh, D. B. Leinweber, A. O Cais and A. G. Williams, Phys. Lett. B **693** (2010) 351.
- [17] R. G. Edwards, J. J. Dudek, D. G. Richards and S. J. Wallace, Phys. Rev. D **84** (2011) 074508.
- [18] C. B. Lang, D. Mohler, S. Prelovsek and M. Vidmar, Phys. Rev. D **84** (2011) 054503.
- [19] S. Prelovsek, C. B. Lang, D. Mohler and M. Vidmar, PoS **LATTICE 2011** (2011) 137.
- [20] Z. Fodor and C. Hoelbling, Rev. Mod. Phys. **84** (2012) 449.
- [21] V. Bernard, U. -G. Meißner and A. Rusetsky, Nucl. Phys. B **788** (2008) 1.
- [22] V. Bernard, M. Lage, U. -G. Meißner, A. Rusetsky, JHEP **0808** (2008) 024.

- [23] M. Doring, U. -G. Meißner, E. Oset and A. Rusetsky, Eur. Phys. J. A **47** (2011) 139.
- [24] M. Lüscher, Commun. Math. Phys. **105** (1986) 153.
- [25] M. Lüscher, Nucl. Phys. B **354** (1991) 531.
- [26] C. Liu, X. Feng and S. He, Int. J. Mod. Phys. A **21** (2006) 847.
- [27] M. Lage, U. -G. Meißner and A. Rusetsky, Phys. Lett. B **681** (2009) 439.
- [28] V. Bernard, M. Lage, U. -G. Meißner and A. Rusetsky, JHEP **1101** (2011) 019.
- [29] M. Doring, J. Haidenbauer, U. -G. Meißner and A. Rusetsky, Eur. Phys. J. A **47**, 163 (2011).
- [30] A. Martinez Torres, L. R. Dai, C. Koren, D. Jido and E. Oset, Phys. Rev. D **85** (2012) 014027.
- [31] M. Doring and U. G. Meißner, JHEP **1201** (2012) 009.
- [32] L. Roca and E. Oset, Phys. Rev. D **85** (2012) 054507.
- [33] J. -J. Xie and E. Oset, arXiv:1201.0149 [hep-ph].
- [34] H. -X. Chen and E. Oset, arXiv:1202.2787 [hep-lat].
- [35] A. Martinez Torres, M. Bayar, D. Jido and E. Oset, arXiv:1202.4297 [hep-lat].
- [36] J. A. Oller, E. Oset and A. Ramos, Prog. Part. Nucl. Phys. **45** (2000) 157.
- [37] J. A. Oller and E. Oset, Phys. Rev. D **60** (1999) 074023.
- [38] J. A. Oller and U. G. Meißner, Phys. Lett. B **500** (2001) 263.
- [39] Z. -H. Guo and J. A. Oller, Phys. Rev. D **84** (2011) 034005.
- [40] T. N. Truong, Phys. Rev. Lett. **61** (1988) 2526; Phys. Rev. Lett. **67** (1991) 2260; A. Dobado *et al.*, Phys. Lett. B **235** (1990) 134; A. Dobado and J. R. Peláez, Phys. Rev. D **47** (1993) 4883; Phys. Rev. D **56** (1997) 3057.
- [41] J. A. Oller, E. Oset and J. R. Peláez, Phys. Rev. D **59** (1999) 074001; [Erratum-ibid. D **60** (1999) 099906]; [Erratum-ibid. D **75** (2007) 099903].
- [42] K. Nakamura *et al.* (Particle Data Group), J. Phys. G **37** (2010) 075021.
- [43] J. A. Oller and E. Oset, Nucl. Phys. A **620** (1997) 438.
- [44] J. Gasser and H. Leutwyler, Annals Phys. **158** (1984) 142.
- [45] E. Oset, A. Ramos and C. Bennhold, Phys. Lett. B **527** (2002) 99.
- [46] A. Gomez Nicola, J. R. Peláez and G. Rios, Phys. Rev. D **77** (2008) 056006.
- [47] C. Hanhart, J. R. Peláez and G. Rios, Phys. Rev. Lett. **100** (2008) 152001.
- [48] G. F. Chew and S. Mandelstam, Phys. Rev. **119** (1960) 467.
- [49] M. Albaladejo and J. A. Oller, Phys. Rev. Lett. **101** (2008) 252002; M. Albaladejo, J. A. Oller and L. Roca, Phys. Rev. D **82** (2010) 094019; M. Albaladejo and J. A. Oller, Phys. Rev. C **84** (2011) 054009; arXiv:1201.0443 [nucl-th].
- [50] A. Lacour, J. A. Oller and U. -G. Meißner, Annals Phys. **326** (2011) 241.
- [51] M. Albaladejo and J. A. Oller, *forthcoming*.
- [52] D. Jido, J. A. Oller, E. Oset, A. Ramos and U. -G. Meißner, Nucl. Phys. A **725** (2003) 181.
- [53] B. Hyams *et al.*, Nucl. Phys. **B64** (1973) 134.
- [54] R. Kaminski, L. Lesniak and K. Rybicki, Z. Phys. C **74** (1997) 79.
- [55] G. Grayer *et al.*, Nucl. Phys. B **75** (1974) 189.
- [56] S. Pislak *et al.* [BNL-E865 Collaboration], Phys. Rev. Lett. **87** (2001) 221801; Phys. Rev. D **67** (2003) 072004.
- [57] L. Masetti [NA48/2 Collaboration], arXiv:hep-ex/0610071.
- [58] M. J. Losty, V. Chaloupka, A. Ferrando, L. Montanet, E. Paul, D. Yaffe, A. Zieminski and J. Alitti *et al.*, Nucl. Phys. B **69** (1974) 185.
- [59] W. Hoogland, S. Peters, G. Grayer, B. Hyams, P. Weillhammer, W. Blum, H. Dietl and G. Hentschel *et al.*, Nucl. Phys. B **126** (1977) 109.